ON THE SAV-DG METHOD FOR A CLASS OF FOURTH ORDER GRADIENT FLOWS *

HAILIANG LIU† AND PEIMENG YIN‡

ABSTRACT. For a class of fourth order gradient flow problems, integration of the scalar auxiliary variable (SAV) time discretization with the penalty-free discontinuous Galerkin (DG) spatial discretization leads to SAV-DG schemes. These schemes are linear and shown unconditionally energy stable. But the reduced linear systems are rather expensive to solve due to the dense coefficient matrices. In this paper, we provide a procedure to pre-evaluate the auxiliary variable in the piecewise polynomial space. As a result the computational complexity of $O(\mathcal{N}^2)$ reduces to $O(\mathcal{N})$ when exploiting the conjugate gradient (CG) solver. This hybrid SAV-DG method is more efficient and able to deliver satisfactory results of high accuracy. This was also compared with solving the full augmented system of the SAV-DG schemes.

1. Introduction

This paper is concerned with efficient numerical approximations to a class of fourth order gradient flows [5]:

$$u_t = -\left(\Delta + \frac{a}{2}\right)^2 u - \Phi'(u), \ x \in \Omega \subset \mathbb{R}^d, \ t > 0, \tag{1.1}$$

which governs the evolution of a scalar time-dependent unknown u = u(x, t) in a convex bounded domain $\Omega \subset \mathbb{R}^d$, Φ is a nonlinear function and a serves as a physical parameter. The model equation (1.1) describes important physical processes in nature. Typical application examples include the Swift-Hohenberg (SH) equation [23] and the extended Fisher-Kolmogorov equation [3, 18].

It is known that under appropriate boundary conditions, equation (1.1) features a decaying free energy

$$\frac{d}{dt}\mathcal{E}(u) = -\int_{\Omega} |u_t|^2 dx \le 0, \tag{1.2}$$

Date: Thursday 3rd August, 2023.

2020 Mathematics Subject Classification. 65N12, 65N30, 35K35.

Key words and phrases. Gradient flows, Swift-Hohenberg equation, energy dissipation, DG method, SAV approach.

★This manuscript has been authored in part by UT-Battelle, LLC, under contract DE-AC05-00OR22725 with the US Department of Energy (DOE). The US government retains and the publisher, by accepting the article for publication, acknowledges that the US government retains a nonexclusive, paid-up, irrevocable, worldwide license to publish or reproduce the published form of this manuscript, or allow others to do so, for US government purposes. DOE will provide public access to these results of federally sponsored research in accordance with the DOE Public Access Plan (http://energy.gov/downloads/doe-public-access-plan).

where

$$\mathcal{E}(u) = \int_{\Omega} \frac{1}{2} (\mathcal{L}u)^2 + \Phi(u) dx, \quad \mathcal{L} = -\left(\Delta + \frac{a}{2}\right). \tag{1.3}$$

This energy dissipation law as a fundamental property of (1.1) is always desirable for numerical approximations, and often crucial to eliminate numerical results that are not physical.

For the spatial discretization, we follow the penalty free discontinuous Galerkin (DG) method introduced in [12]. The key idea is to introduce $q = \mathcal{L}u$ so that the resulting semi-discrete DG scheme becomes

$$(u_{ht}, \phi) = -A(q_h, \phi) - (\Phi'(u_h), \phi),$$
 (1.4a)

$$(q_h, \psi) = A(u_h, \psi), \tag{1.4b}$$

for all ϕ , ψ in the same DG space as for u_h, q_h . Here $A(q_h, \cdot)$ is the DG discretization of $(\mathcal{L}q, \cdot)$. This spatial DG discretization avoids the use of penalty parameters (called penalty-free DG method) in the numerical flux on interior cell interfaces. It also inherits most of the advantages of the usual DG methods (see e.g. [10, 19, 20]), such as high order accuracy, flexibility in hp-adaptation, capacity to handle domains with complex geometry.

In order to formulate an energy dissipative scheme with the time discretization, the linear terms in (1.4) can be treated implicitly, but nonlinear terms have to be handled with care. The IEQ-DG method introduced in [13] is to integrate the DG method with the method of invariant energy quadratization (IEQ) [24, 27]. It boils down to solving an augmented system involving the dynamics of the auxiliary variable $U = \sqrt{\Phi(u_h) + B}$. We remark that the IEQ approach is remarkable as it allows one to construct linear, unconditionally energy stable schemes for a large class of gradient flows (see, e.g. [24, 25, 26, 27, 13, 14]). We refer the readers to [13] for more references to earlier results on both the DG approximation and the time discretization.

As pointed out in [13], one could also integrate the same DG method with the so-called SAV approach [21] by introducing an auxiliary variable $r = \sqrt{\int_{\Omega} \Phi(u(x,t)) dx + B}$. This transforms (1.4) into another augmented system. As for the IEQ-DG method, here one can also obtain a closed linear system for (u_h^{n+1}, q_h^{n+1}) only. Unfortunately, such systems involve dense coefficient matrices and rather expensive to solve.

There are two ways to get around this obstacle: (i) find a path to lower the computational complexity of solving the reduced linear system; or (ii) return to the full augmented system with $(u_h^{n+1}, q_h^{n+1}, r^{n+1})$ as unknowns. For (i) we introduce a special procedure to pre-compute $r^{n+1} = r(t^{n+1})$ in the piecewise polynomial space based on a linear DG solver; with such obtained r^{n+1} , we solve the SAV-DG schemes with reduced computational cost. This treatment is interesting in its own sake. We name it the hybrid SAV-DG method. For (ii), the full augmented system indeed involves only sparse coefficient matrices. Here the full system contains one more equation since r does not depend on r. In contrast, the full system with $(u_h^{n+1}, q_h^{n+1}, U^{n+1})$ as unknowns for the IEQ-DG method contains N(k+1) more equations. Here r is the total number of the 1-D meshes, and r the degree of DG polynomials. The advantage of the IEQ-DG method lies in the simplicity of its reduced system.

Comparing the linear systems of the above three SAV-DG type-schemes, we see that the coefficient matrices are all symmetric, but it is time-dependent and dense for the reduced system, time-dependent and sparse for the full augmented system, and time-independent and sparse for the hybrid SAV-DG. Indeed, our numerical tests confirm that the hybrid SAV-DG algorithm performs the best. The SAV approach may also be integrated with other DG methods in such hybrid manner.

Due to recent works (see, e.g., [1, 7, 8, 9]) both IEQ and SAV approaches could also be made arbitrarily high order in time. Though here we only discuss first and second order time discretization with the SAV approach, an extension to SAV-DG schemes of arbitrary high order (in time) is possible. For ODE solvers on such extension we refer to [15], where arbitrarily high order IEQ-based RKDG schemes are constructed to solve equations of form (1.1).

As for the spatial discretization of (1.1), one may also adopt other methods such as the pseudo-spectral method [11, 28] to capture spatial patterns with high-resolution on structured meshes, while extra issues are involved when dealing with complex domains or non-periodic boundary conditions. The main purpose of this work is to show how to integrate the SAV approach with the DG spatial discretization, in contrast to collocation methods studied in [21, 1, 7, 8, 9] for either SAV or IEQ schemes.

1.1. **Organization.** This paper is organized as follows: In Section 2, we formulate a unified semi-discrete DG method for the fourth order equation (1.1) subject to two different boundary conditions. In Section 3, we present SAV-DG schemes, show the energy dissipation law, and discuss several ways to efficiently implement the schemes. In Section 4, we provide a procedure to pre-evaluate the auxiliary variable and then present the according algorithms. In Section 5, we verify the good performance of the hybrid SAV-DG using several numerical examples. Finally some concluding remarks are given in Section 6.

Notation: Throughout this paper, we use the notation Π to indicate the usual piecewise L^2 projection in the sense of inner product with $\forall \phi \in V_h$,

$$(\Pi w, \phi) = (w, \phi), \quad \forall \phi \in V_h,$$

where V_h is the discontinuous Galerkin finite element space.

2. Spatial DG discretization

To introduce the hybrid SAV-DG algorithm, we need to first recall some conventions about the semi-discrete DG discretization introduced in [12]. To be specific, we only consider homogeneous boundary conditions of form

(i)
$$u$$
 is periodic; or (ii) $\partial_{\mathbf{n}} u = \partial_{\mathbf{n}} \Delta u = 0, \quad x \in \partial \Omega,$ (2.1)

where **n** stands for the unit outward normal to the boundary $\partial\Omega$.

For the fourth order PDE (1.1), we set $q = \mathcal{L}u$ so that the model admits the following mixed form

$$\begin{cases} u_t = -\mathcal{L}q - \Phi'(u), \\ q = \mathcal{L}u. \end{cases}$$
 (2.2)

Let the domain Ω be a union of shape regular meshes $\mathcal{T}_h = \{K\}$, with the mesh size $h_K = \text{diam}\{K\}$ and $h = \max_K h_K$. We denote the set of the interior interfaces by Γ^0 , the set of all boundary faces by Γ^{∂} , and the discontinuous Galerkin finite element space by

$$V_h = \{ v \in L^2(\Omega) : v|_K \in P^k(K), \ \forall K \in \mathcal{T}_h \},$$

where $P^k(K)$ denotes the set of polynomials of degree no more than k on element K. If the normal vector on the element interface $e \in \partial K_1 \cap \partial K_2$ is oriented from K_1 to K_2 , then the average $\{\cdot\}$ and the jump $[\cdot]$ operator are defined by

$$\{v\} = \frac{1}{2}(v|_{\partial K_1} + v|_{\partial K_2}), \quad [v] = v|_{\partial K_2} - v|_{\partial K_1},$$

for any function $v \in V_h$, where $v|_{\partial K_i}$ (i = 1, 2) is the trace of v on e evaluated from element K_i . Then the DG method for (2.2) is to find $(u_h(\cdot, t), q_h(\cdot, t)) \in V_h \times V_h$ such that

$$(u_{ht}, \phi) = -A(q_h, \phi) - (\Phi'(u_h), \phi),$$
 (2.3a)

$$(q_h, \psi) = A(u_h, \psi), \tag{2.3b}$$

for all ϕ , $\psi \in V_h$. The initial data for u_h is taken as the piecewise L^2 projection, denoted by $u_h(x,0) = \Pi u_0(x)$. In the above scheme formulation $A(q_h,\phi)$ is the DG discretization of $(\mathcal{L}q,\phi)$ and $A(u_h,\psi)$ is the DG discretizationvof $(\mathcal{L}u,\psi)$.

The precise form of $A(\cdot,\cdot)$ depending on the types of boundary conditions is given as follows:

$$A(w, v) = A^{0}(w, v) + A^{b}(w, v)$$

with

$$A^{0}(w,v) = \sum_{K \in \mathcal{T}} \int_{K} \left(\nabla w \cdot \nabla v - \frac{a}{2} wv \right) dx + \sum_{e \in \Gamma^{0}} \int_{e} \left(\{ \partial_{\nu} w \}[v] + [w] \{ \partial_{\nu} v \} \right) ds. \tag{2.4}$$

Here $A^b(\cdot,\cdot)$ are given below for each respective type of boundary conditions:

for (i) of (2.1)
$$A^{b}(w,v) = \frac{1}{2} \int_{\Gamma^{\partial}} (\{\partial_{\nu}w\}[v] + [w]\{\partial_{\nu}v\}) ds, \qquad (2.5a)$$

for (ii) of (2.1)
$$A^b(w, v) = 0.$$
 (2.5b)

Note that for periodic case in (2.5a) the left boundary and the right boundary are considered as same, for which we use the factor 1/2 to avoid recounting.

One can verify that the semi-discrete scheme (2.3) satisfies a discrete energy dissipation law (see [13])

$$\frac{d}{dt}\mathcal{E}(u_h, q_h) = -\int_{\Omega} |u_{ht}|^2 dx \le 0,$$

where

$$\mathcal{E}(u_h, q_h) = \int_{\Omega} \frac{1}{2} |q_h|^2 + \Phi(u_h) dx.$$
 (2.6)

For non-homogeneous boundary conditions, it only requires a modification by adding some source terms in the DG formulation. Of course, the energy dissipation also needs to be refined to account for the boundary effects.

3. Time discretization

With time discretization using the SAV approach (cf. [21]), we introduce

$$r = r(t) := \sqrt{\int_{\Omega} \Phi(u_h(x,t)) dx + B}$$

where B is so chosen that this quantity is well-defined, and consider the following enlarged system: find $(u_h(\cdot,t),q_h(\cdot,t)) \in V_h \times V_h$ and r=r(t) such that

$$(u_{ht}, \phi) = -A(q_h, \phi) - r(b(u_h), \phi),$$
 (3.1a)

$$(q_h, \psi) = A(u_h, \psi), \tag{3.1b}$$

$$r_t = \frac{1}{2} \int_{\Omega} b(u_h) u_{ht} dx, \tag{3.1c}$$

for all $\phi, \psi \in V_h$. Here we use the notation

$$b(w(\cdot)) = \frac{\Phi'(w(\cdot))}{\sqrt{\int_{\Omega} \Phi(w(x))dx + B}}.$$
(3.2)

The initial data for the above scheme is chosen as

$$u_h(x,0) = \Pi u_0(x), \quad r(0) = \sqrt{\int_{\Omega} \Phi(u_0(x)) dx + B},$$

where Π denotes the piecewise L^2 projection into V_h .

One can verify that a modified energy of form

$$E(u_h, q_h, r) = \frac{1}{2} \int_{\Omega} q_h^2 dx + r^2 = \mathcal{E}(u_h, q_h) + B$$
(3.3)

satisfies the following dissipation inequality

$$\frac{d}{dt}E(u_h, q_h, r) = -\int_{\Omega} |u_{ht}|^2 dx \le 0.$$

Using the Euler-forward time discretization, we obtain the first order SAV-DG scheme: find $(u_h^n, q_h^n) \in V_h \times V_h$ and $r^n = r(t^n)$ such that for any for $\phi, \psi \in V_h$,

$$(D_t u_h^n, \phi) = -A(q_h^{n+1}, \phi) - r^{n+1} (b(u_h^n), \phi),$$
(3.4a)

$$(q_h^n, \psi) = A(u_h^n, \psi), \tag{3.4b}$$

$$D_t r^n = \frac{1}{2} \int_{\Omega} b(u_h^n) D_t u_h^n dx, \tag{3.4c}$$

The initial data $u_h^0 = u_h(x,0)$, $r^0 = r(0)$. Here we used $D_t v^n = \frac{v^{n+1} - v^n}{\Delta t}$.

Reformulation (3.1) also allows for even higher order in time discretization. To illustrate this we only consider a second order SAV-DG scheme: find $(u_h^n, q_h^n) \in V_h \times V_h$ such that for for all

 $\phi, \psi \in V_h$

$$(D_t u_h^n, \phi) = -A(q_h^{n+1/2}, \phi) - r^{n+1/2} (b(u_h^{n,*}), \phi), \qquad (3.5a)$$

$$(q_h^n, \psi) = A(u_h^n, \psi), \tag{3.5b}$$

$$D_t r^n = \frac{1}{2} \int_{\Omega} b(u_h^{n,*}) D_t u_h^n dx, \qquad (3.5c)$$

where $v^{n+1/2} = (v^n + v^{n+1})/2$ for $v = u_h, q_h, r$, and $u_h^{n,*}$ is defined by

$$u_h^{n,*} = \frac{3}{2}u_h^n - \frac{1}{2}u_h^{n-1}. (3.6)$$

Here instead of $u_h^{n+1/2}$ we use $u_h^{n,*}$ to avoid the use of iteration steps in updating the numerical solution, while still maintaining second order accuracy in time. When n=0 in (3.6), we simply take $u_h^{-1}=u_h^0$.

Both scheme (3.4) and (3.5) are unconditionally energy stable.

Theorem 3.1. (i) Scheme (3.4) admits a unique solution (u_h^n, q_h^n) , and for $E^n := E(u_h^n, q_h^n, r^n)$, we have

$$E^{n+1} = E^n - \frac{\|u_h^{n+1} - u_h^n\|^2}{\Delta t} - \frac{1}{2} \|q_h^{n+1} - q_h^n\|^2 - |r^{n+1} - r^n|^2.$$
(3.7)

for any $\Delta t > 0$.

(ii) Scheme (3.5) admits a unique solution, and

$$E^{n+1} = E^n - \frac{\|u_h^{n+1} - u_h^n\|^2}{\Delta t}$$
(3.8)

for any $\Delta t > 0$.

The proof of this result is deferred to Appendix A.

Though SAV-DG schemes are linear and unconditionally energy stable, their numerical implementations cannot be handled as for the IEQ-DG schemes in [13]. To see this, we follow [13] to rewrite (3.4) into a closed linear system for (u_h^{n+1}, q_h^{n+1}) as

$$\left(u_{h}^{n+1}, \phi\right) + \frac{\Delta t}{2} \left(b(u_{h}^{n}), \phi\right) \left(b(u_{h}^{n}), u_{h}^{n+1}\right) + \Delta t A(q_{h}^{n+1}, \phi)
= \left(u_{h}^{n}, \phi\right) + \frac{\Delta t}{2} \left(b(u_{h}^{n}), \phi\right) \left(b(u_{h}^{n}), u_{h}^{n}\right) - r^{n} \left(b(u_{h}^{n}), \phi\right),
A(u_{h}^{n+1}, \psi) - \left(q_{h}^{n+1}, \psi\right) = 0.$$
(3.9)

This linear system with a nonlocal term $(b(u_h^n), u_h^{n+1})$ has a symmetric yet dense and unstructured coefficient matrix, and is rather expensive to solve.

To get around this obstacle, we either return to the augmented system with $(u_h^{n+1}, q_h^{n+1}, r^{n+1})$ as unknowns, or attempt to find a way to reduce the computational complexity of solving the reduced linear system (3.9). For the former, the linear system for the first order scheme is

$$(\Delta t)^{-1} (u_h^{n+1}, \phi) + A(q_h^{n+1}, \phi) + r^{n+1} (b(u_h^n), \phi) = (\Delta t)^{-1} (u_h^n, \phi),$$
(3.10a)

$$A(u_h^{n+1}, \psi) - (q_h^{n+1}, \psi) = 0, \tag{3.10b}$$

$$(u_h^{n+1}, b(u_h^n)) - 2r^{n+1} = (u_h^n, b(u_h^n)) - 2r^n.$$
(3.10c)

Though the coefficient matrix of this linear system is also time-dependent, it is sparse and symmetric, hence still suitable for efficient computing. In fact, we use the conjugate gradient (CG) solver to solve this system with the computational complexity of order $O(\mathcal{N})$; while it is of order $O(\mathcal{N}^2)$ when solving the reduced system (3.9); see, e.g., [22].

As for the latter, we introduce a special procedure to pre-compute r^{n+1} in order to substantially reduce the total computational complexity. This treatment is interesting in particular within the DG framework. The details will be presented in the next section. For a class of Cahn-Hillard type gradient flows, the authors of [21] suggested a procedure for the SAV approach at the semi-discrete level, which involves in solving two fourth-order elliptic equations sequentially. However, solving fourth-order equations within the DG framework can be a challenging task. Our pre-evaluation to be detailed in Section 4 provides novel techniques for actually implementing a fully-discrete SAV-DG method.

4. Pre-evaluation of the auxiliary variable and algorithms

4.1. **Pre-evaluation of the auxiliary variable** r^{n+1} . We introduce an auxiliary linear system: find $(v_h, w_h) \in V_h \times V_h$ such that for $\forall \phi, \psi \in V_h$,

$$\tau A(w_h, \phi) + (v_h, \phi) = (f_h, \phi),$$

$$(w_h, \psi) = A(v_h, \psi),$$
(4.1)

and define operator $(\mathcal{L}_h v, \psi) = A(v, \psi)$ for any $\psi \in V_h$. We have the following.

Lemma 4.1. For any $\tau > 0$ and f_h given, system (4.1) admits a unique solution (v_h, w_h) , given by

$$v_h = \mathcal{B}_h(\tau) f_h, \quad w_h = \mathcal{L}_h v_h = \mathcal{L}_h \mathcal{B}_h(\tau) f_h.$$
 (4.2)

Moreover, the operator $\mathcal{B}_h(\tau)$ can be expressed as $(I + \tau \mathcal{L}_h^2)^{-1}$, with the following bounds:

$$(f_h, \mathcal{B}_h(\tau)f_h) = \|\mathcal{B}_h(\tau)f_h\|^2 + \tau \|\mathcal{L}_h \mathcal{B}_h(\tau)f_h\| \ge 0.$$

$$\|\mathcal{B}_h(\tau)f_h\| < \|f_h\|.$$
(4.3)

Proof. Set $\phi = v_h$ and $\psi = w_h$ in (4.1) so that

$$||v_h||^2 + \tau ||w_h||^2 = (f_h, v_h) \le \frac{1}{2} (||f_h||^2 + ||v_h||^2).$$

Hence

$$||v_h||^2 + 2\tau ||w_h||^2 \le ||f_h||^2. \tag{4.4}$$

This a priori estimate ensures both existence and uniqueness of the linear system (4.1). Combining two equations in (4.1) we obtain

$$(\tau \mathcal{L}_h^2 + I)v_h = f_h.$$

This implies that

$$\mathcal{B}_h(\tau) = (I + \tau \mathcal{L}_h^2)^{-1}$$

and (4.3) follows from (4.4), completing the proof.

Equipped with the above result, we can compute r^{n+1} in advance for the SAV-DG scheme (3.4).

Theorem 4.1. Givn (u_h^n, q_h^n) , scheme (3.4) can be realized in two steps:

(i) Determine r^{n+1} by

$$r^{n+1} = r^n - \frac{1}{2}(\Pi b(u_h^n), u_h^n) + \frac{1}{2}R^n, \tag{4.5}$$

where

$$R^{n} = \frac{(b(u_{h}^{n}), \mathcal{B}_{h}(\Delta t)\xi^{n})}{1 + \frac{\Delta t}{2}(\Pi b(u_{h}^{n}), \mathcal{B}_{h}(\Delta t)\Pi b(u_{h}^{n}))},$$

$$(4.6)$$

$$\xi^{n} = u_{h}^{n} - \Delta t \Pi b(u_{h}^{n}) r^{n} + \frac{\Delta t}{2} \Pi b(u_{h}^{n}) \left(b(u_{h}^{n}), u_{h}^{n} \right); \tag{4.7}$$

(ii) with such obtained r^{n+1} we solve the following linear system:

$$(D_t u_h^n, \phi) = -A(q_h^{n+1}, \phi) - (b(u_h^n), \phi) r^{n+1},$$

$$(q_h^{n+1}, \psi) = A(u_h^{n+1}, \psi).$$

Proof. Denote $\mathcal{B}_h = \mathcal{B}_h(\Delta t)$. From (3.4a) we have

$$u_h^{n+1} = u_h^n - \Delta t \mathcal{L}_h^2 u_h^{n+1} - \Delta t \Pi b(u_h^n) r^{n+1} \in V_h, \tag{4.8}$$

which further gives

$$u_h^{n+1} = \mathcal{B}_h u_h^n - \Delta t r^{n+1} \mathcal{B}_h \Pi b(u_h^n).$$

Using (3.4c), i.e.,

$$r^{n+1} = r^n + \frac{1}{2} \left(b(u_h^n), u_h^{n+1} - u_h^n \right), \tag{4.9}$$

we see that

$$u_h^{n+1} = \mathcal{B}_h \xi^n - \frac{\Delta t}{2} \mathcal{B}_h \Pi b(u_h^n) \left(b(u_h^n), u_h^{n+1} \right),$$

where ξ^n is given in (4.7). Applying inner product against $b(u_h^n)$ gives

$$\left(1 + \frac{\Delta t}{2} \left(b(u_h^n), \mathcal{B}_h \Pi b(u_h^n)\right)\right) \left(b(u_h^n), u_h^{n+1}\right) = \left(b(u_h^n), \mathcal{B}_h \xi^n\right).$$

Since $(\mathcal{B}_h \Pi b(u_h^n), b(u_h^n)) = (\mathcal{B}_h \Pi b(u_h^n), \Pi b(u_h^n)) \ge 0$, hence,

$$\left(b(u_h^n), u_h^{n+1}\right) = \frac{\left(b(u_h^n), \mathcal{B}_h \xi^n\right)}{1 + \frac{\Delta t}{2} \left(\Pi b(u_h^n), \mathcal{B}_h \Pi b(u_h^n)\right)}.$$

This when inserted into (4.9) completes the proof.

We can also compute r^{n+1} in advance for the second order SAV-DG scheme (3.5).

Theorem 4.2. Given (u_h^n, q_h^n) , scheme (3.5) can be realized in two steps:

(i) Determine $r^{n+1/2}$ by

$$r^{n+1/2} = r^n - \frac{1}{2}(\Pi b(u_h^{n,*}), u_h^n) + \frac{1}{2}R^{n,*}, \tag{4.10}$$

where

$$R^{n,*} = \frac{(b(u_h^{n,*}), \mathcal{B}_h(\Delta t/2)\xi^{n,*})}{1 + \frac{\Delta t}{4} (\Pi b(u_h^{n,*}), \mathcal{B}_h(\Delta t/2)\Pi b(u_h^{n,*}))}, \tag{4.11}$$

$$\xi^{n,*} = u_h^n - \frac{1}{2} \Delta t r^n \Pi b(u_h^{n,*}) + \frac{\Delta t}{4} \Pi b(u_h^{n,*}) \left(b(u_h^{n,*}), u_h^n \right); \tag{4.12}$$

(ii) with such obtained $r^{n+1/2}$ we solve the following linear system:

$$(D_t u_h^n, \phi) = -A(q_h^{n+1/2}, \phi) - (b(u_h^{n,*}), \phi) r^{n+1/2},$$

$$(q_h^n, \psi) = A(u_h^n, \psi).$$
(4.13)

Proof. Scheme (3.5) may be rewritten as

$$\begin{split} \left(\tilde{D}_t u_h^{n+1/2}, \phi \right) &= -A(q_h^{n+1/2}, \phi) - r^{n+1/2} \left(b(u_h^{n,*}), \phi \right), \\ \left(q_h^n, \psi \right) &= A(u_h^n, \psi), \\ \tilde{D}_t r^{n+1/2} &= \frac{1}{2} \int_{\Omega} b(u_h^{n,*}) \tilde{D}_t u_h^{n+1/2} dx, \end{split}$$

Here \tilde{D}_t denotes a forward difference with time step $\Delta t/2$ so that

$$\tilde{D}_t r^{n+1/2} = D_t r^n.$$

This is the same form as the first order SAV-DG method with $b(u_h^n)$ replaced by $b(u_h^{n,*})$ and time step Δt replaced by $\Delta t/2$. Hence the claimed results follow directly from those in Theorem 4.1.

4.2. **Algorithms.** The details related to the scheme implementation are summarized in the following algorithms.

Algorithm 4.1. Hybrid algorithm for the first order SAV-DG scheme (3.4).

- Step 1 (Initialization) From the given initial data $u_0(x)$
 - (1) generate $u_h^0 = \Pi u_0(x) \in V_h$;
 - (2) generate $r^0 = \sqrt{\int_{\Omega} \Phi(u_0(x)) dx + B}$, where B is a priori chosen constant so that $\inf_v(\int_{\Omega} \Phi(v(x)) dx + B) > 0$.
- Step 2 (Evolution)
 - (1) solve for $\Pi b(u_h^n)$ from $b(u_h^n)$;
 - (2) obtain $\mathcal{B}_h(\Delta t)\Pi b(u_h^n) = v_h$ by solving the linear system (4.1) with $f_h = \Pi b(u_h^n)$;
 - (3) obtain $\mathcal{B}_h(\Delta t)\xi^n = v_h$ by solving the linear system (4.1) with $f_h = \xi_n$ in (4.7);
 - (4) calculate R^n in (4.6);
 - (5) calculate r^{n+1} through (4.5);
 - (6) solve the following linear system for u_h^{n+1}, q_h^{n+1} ,

$$(u_h^{n+1}, \phi) + \Delta t A(q_h^{n+1}, \phi) = (u_h^n, \phi) - \Delta t (b(u_h^n), \phi) r^{n+1}$$

$$A(u_h^{n+1}, \psi) - (q_h^{n+1}, \psi) = 0.$$

Algorithm 4.2. Hybrid algorithm for the second order SAV-DG scheme (3.5).

- Step 1 (Initialization) From the given initial data $u_0(x)$
 - (1) generate $u_h^0 = \Pi u_0(x) \in V_h$;
 - (2) solve for q_h^0 from (3.5b) based on u_h^0 ;
 - (3) generate $r^0 = \sqrt{\int_{\Omega} \Phi(u_0(x)) dx} + B$, where B is a priori chosen constant so that $\inf_v(\int_{\Omega} \Phi(v(x)) dx + B) > 0$.

- Step 2 (Evolution)
 - (1) solve for $\Pi b(u_h^{n,*})$ based on $b(u_h^{n,*})$, where $u_h^{n,*}$ is defined in (3.6);
 - (2) obtain $\mathcal{B}_h(\Delta t/2)\Pi b(u_h^{n,*}) = v_h$ by solving the linear system (4.1) with $f_h = \Pi b(u_h^{n,*})$;
 - (3) obtain $\mathcal{B}_h(\Delta t/2)\xi^{n,*} = v_h$ by solving the linear system (4.1) with $f_h = \xi^{n,*}$ in (4.12);
 - (4) calculate $R^{n,*}$ in (4.11);
 - (5) calculate $r^{n+1/2}$ through (4.10);
 - (6) solve the following linear system for $u_h^{n+1/2}, q_h^{n+1/2},$

$$\left(u_h^{n+1/2}, \phi \right) + (\Delta t/2) A(q_h^{n+1/2}, \phi) = (u_h^n, \phi) - (\Delta t/2) \left(b(u_h^{n,*}), \phi \right) r^{n+1/2},$$

$$A(u_h^{n+1/2}, \psi) - (q_h^{n+1/2}, \psi) = 0;$$

(7) calculate $u_h^{n+1} = 2u_h^{n+1/2} - u_h^n$.

Note that each coefficient matrix of the linear system involved in Algorithm 4.1 and 4.2 is symmetric, sparse and time-independent. The use of the CG solver for solving these linear systems induces the computational complexity of only order $O(\mathcal{N})$.

5. Numerical examples

In this section we numerically test both the spatial and temporal orders of convergence, and apply the second order fully discrete SAV-DG scheme (3.5) to recover roll patterns and hexagonal patterns governed by the two dimensional Swift-Hohenberg equation and further verify the unconditional energy stability of the numerical solutions.

In our numerical tests, we take rectangular meshes. The L^{∞} and L^2 errors between the numerical solution $u_h^n(x,y)$ and the exact solution $u(t^n,x,y)$ evaluated to obtain experimental orders of convergence (EOC) are defined respectively by

$$e^n_h = \max_i \max_{0 \le l \le k+1} \max_{0 \le s \le k+1} |u^n_h(\hat{x}^i_l, \hat{y}^i_s) - u(t^n, \hat{x}^i_l, \hat{y}^i_s)|$$

and

$$e_h^n = \left(\sum_i \frac{h_x^i h_y^i}{4} \sum_{l=1}^{k+1} \sum_{s=1}^{k+1} \omega_{l,s} |u_h^n(\hat{x}_l^i, \hat{y}_s^i) - u(t^n, \hat{x}_l^i, \hat{y}_s^i)|^2\right)^{1/2},$$

where $\omega_{l,s} > 0$ are the weights, and $(\hat{x}_l^i, \hat{y}_s^i)$ are the corresponding quadrature points. The EOC at $T = n\Delta t = 2n(\Delta t/2)$ in terms of mesh size $h = \max_i \{h_x^i, h_y^i\}$ and time step Δt are calculated respectively by

$$EOC = \log_2\left(\frac{e_h^n}{e_{h/2}^n}\right), \quad EOC = \log_2\left(\frac{e_h^n}{e_h^{2n}}\right).$$

The relative errors in L^{∞} and L^2 norm are defined respectively by

$$\frac{\|u_h^n(x,y) - u(t^n,x,y)\|_{L^{\infty}(\Omega)}}{\|u(t^n,x,y)\|_{L^{\infty}(\Omega)}} \quad \text{and} \quad \frac{\|u_h^n(x,y) - u(t^n,x,y)\|}{\|u(t^n,x,y)\|}.$$

The Swift-Hohenberg equation is a special case of model equation (1.1) with a=2 and

$$\Psi(u) = \frac{1 - \epsilon}{2}u^2 - \frac{g}{3}u^3 + \frac{u^4}{4},$$

that is,

$$u_t = -\Delta^2 u - 2\Delta u + (\epsilon - 1)u + gu^2 - u^3.$$
 (5.1)

Here physical parameters are $g \ge 0$ and ϵ , which together with the size of the domain play an important role in pattern selection; see, e.g., [2, 17, 16]. Our numerical tests center on this equation for which

$$\Phi(u) = -\frac{\epsilon}{2}u^2 - \frac{g}{3}u^3 + \frac{u^4}{4}$$

and $g \ge 0$ and $\epsilon > 0$. This function has double wells with two local minimal values at $u_{\pm} = \frac{g \pm \sqrt{g^2 + 4\epsilon}}{2}$ such that $\Phi'(u_{\pm}) = 0$, and

$$\Phi(u) \ge \min\{\Phi(u_{\pm})\} = \min_{v=u_{\pm}} \left(-\frac{1}{12} \left(gv(g^2 + 4\epsilon) + \epsilon(g^2 + 3\epsilon) \right) \right) = -a,$$

so it suffices to choose the method parameter $B = a|\Omega|$. In all numerical examples a < 1, so we simply take $B = |\Omega|$ for all cases.

Example 5.1. (Spatial Accuracy Test) Consider the Swift-Hohenberg equation (5.1) with an added source of form

$$f(x, y, t) = -\varepsilon v - gv^2 + v^3, \quad v := e^{-t/4} \sin(x/2) \sin(y/2),$$

on Ω , subject to initial data

$$u_0(x,y) = \sin(x/2)\sin(y/2), \quad (x,y) \in \Omega.$$
 (5.2)

This problem has an explicit solution

$$u(x, y, t) = e^{-t/4} \sin(x/2) \sin(y/2), \quad (x, y) \in \Omega.$$
 (5.3)

This example is used to test the spatial accuracy, using polynomials of degree k with k = 1, 2, 3 on 2D rectangular meshes. In the second-order SAV-DG scheme (3.5), we need to add

$$\frac{1}{2}\left(f(\cdot,t^{n+1},\phi)+f(\cdot,t^n,\phi)\right),\,$$

to the right hand side of (3.5a).

Test case 1. We take $\varepsilon = 0.025, g = 0$, and domain $\Omega = [-2\pi, 2\pi]^2$ with periodic boundary conditions. Both errors and orders of convergence at T = 0.01 are reported in Table 1. These results confirm the (k+1)th orders of accuracy in L^2, L^∞ norms.

Test case 2. We take $\varepsilon = 0.025, g = 0.05$, domain $\Omega = [-\pi, 3\pi]^2$ with boundary condition $\partial_{\nu}u = \partial_{\nu}\Delta u = 0$, $(x, y) \in \partial\Omega$. Both errors and orders of convergence at T = 0.01 are reported in Table 2. These results also show that (k+1)th orders of accuracy in both L^2 and L^{∞} norms are obtained.

Example 5.2. (Temporal Accuracy Test) Consider the Swift-Hohenberg equation with source term given as in Example 5.1. We take $\varepsilon = 0.025$ and g = 0, and domain $\Omega = [-4\pi, 4\pi]^2$ with periodic boundary conditions, subject to initial data

$$u_0(x,y) = \sin(x/4)\sin(y/4).$$
 (5.4)

12 H. LIU, P. YIN

Table 1. L^2, L^{∞} errors and EOC at T=0.01 with mesh $N\times N$.

N=8 N=16 N=32 N=64

$ _{k}$	Δt		N=8	N=16		N=32		N=64	
			error		order		order		order
1	10.3	$ u-u_h _{L^2}$	3.18621e-01	8.28732e-02	1.94	2.02935e-02	2.03	5.04416e-03	2.01
	16-9	$ u-u_h _{L^{\infty}}$	1.38452e-01	3.83881e-02	1.85	2.02935e-02 9.61389e-03	2.00	2.40363e-03	2.00
2	1e-4	$ u-u_h _{L^2}$	6.96867e-02	1.49828e-02	2.22	2.01641e-03 4.02470e-04	2.89	2.56761e-04	2.97
		$ u-u_h _{L^{\infty}}$	2.41046e-02	2.94730e-03	3.03	4.02470e-04	2.87	5.14111e-05	2.97
2	1e-5	$ u-u_h _{L^2}$	1.19940e-02	1.13110e-03	3.41	7.72013e-05 2.43503e-05	3.87	5.01113e-06	3.95
		$ u-u_h _{L^{\infty}}$	3.85634e-03	3.68735e-04	3.39	2.43503e-05	3.92	1.53912e-06	3.98

Table 2. L^2, L^∞ errors and EOC at T=0.01 with mesh $N\times N$.

$ _{k}$	Δt		N=8	N=16		N=32		N=64	
			error		order		order		order
1	10.3	$ u-u_h _{L^2}$	3.18621e-01	8.28732e-02	1.94	2.02935e-02	2.03	5.04416e-03	2.01
	16-9	$ u-u_h _{L^{\infty}}$	1.38452e-01	3.83886e-02	1.85	9.61391e-03	2.00	5.04416e-03 2.40363e-03	2.00
2		$ u-u_h _{L^2}$	6.96867e-02	1.49828e-02	2.22	2.01641e-03	2.89	2.56762e-04 5.14110e-05	2.97
2	1e-5	$ u-u_h _{L^2}$	1.19940e-02	1.13110e-03	3.41	7.72042e-05	3.87	5.05657e-06 1.53917e-06	3.93
		$ u-u_h _{L^{\infty}}$	3.85659e-03	3.68738e-04	3.39	2.43504e-05	3.92	1.53917e-06	3.98

Its exact solution is given by

$$u(x, y, t) = e^{-49t/64} \sin(x/4) \sin(y/4), \quad (x, y) \in \Omega.$$

Test case 1. We compute the numerical solutions using the SAV-DG schemes (3.4) and (3.5) based on P^2 polynomials with time steps $\Delta t = 2^{-m}$ for $2 \le m \le 5$ and mesh size 64×64 . The L^2, L^∞ errors and orders of convergence at T = 2 are shown in Table 3, and these results confirm that DG schemes (3.4) and (3.5) are first order and second order in time, respectively.

Table 3. L^2, L^{∞} errors and EOC at T=2 with time step Δt .

Scheme	Mosh		$\Delta t = 2^{-2}$	$\Delta t = 2^{-3}$		$\Delta t = 2^{-4}$		$\Delta t = 2^{-5}$	
			error		order		order		order
(3.4)	64×64	$ u-u_h _{L^2}$	3.05892e-01	1.58442e-01	0.95	8.07023e-02	0.97	4.07442e-02	0.99
(3.4)		$ u-u_h _{L^{\infty}}$	1.75153e-02	9.09087e-03	0.95	4.64080e-03	0.97	2.34881e-03	0.98
(3.5)	64×64	$ u-u_h _{L^2}$	4.17744e-02	8.14437e-03	2.36	1.74312e-03	2.22	3.98404e-04	2.13
(3.3)		$ u-u_h _{L^{\infty}}$	4.01428e-03	7.92985e-04	2.34	1.46602e-04	2.44	3.60847e-05	2.02

Test case 2. Again, we compute the numerical solutions using the SAV-DG scheme (3.5) based on P^2 polynomials with time steps $\Delta t = 2^{-m}$ for $2 \le m \le 5$ and mesh size $N \times N$ with N = 32 and N = 64. The evolution of the relative L^2 and L^{∞} errors of the numerical solution with different time steps is shown in Figure 1. We also show the evolution of the difference $u_h^n(x, y) - u(t^n, x, y)$

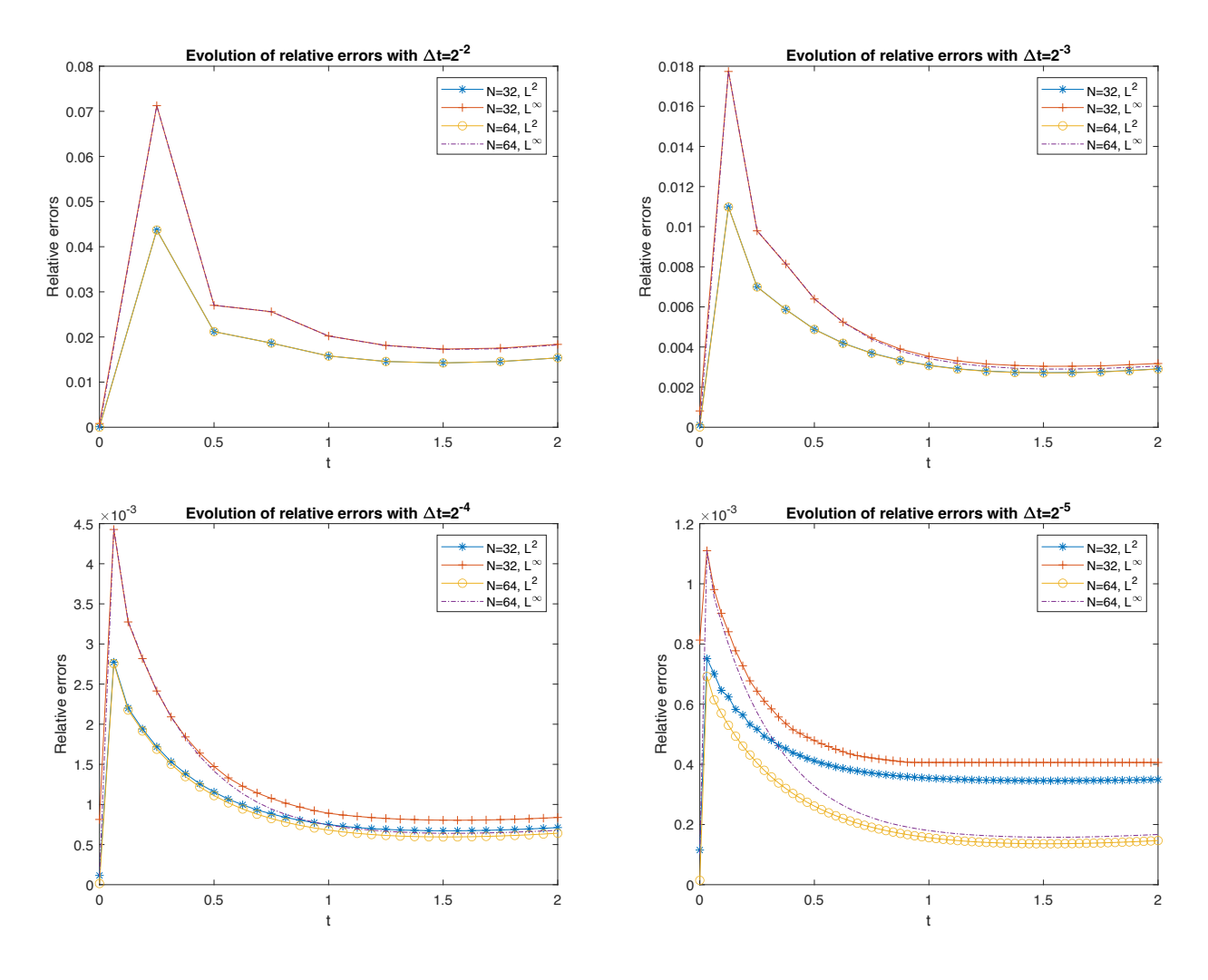


FIGURE 1. Evolution of relative errors with different time step.

with mesh size 64×64 and different time steps. For $\Delta t = 2^{-2}$ and $\Delta t = 2^{-5}$, the evolution is shown in Figure 2 and Figure 3, respectively. All these results indicate that the SAV-DG method is able to keep the desired accuracy of the numerical solution over long time simulation.

Example 5.3. We consider the Swift-Hehenberg equation with the parameters in Example 5.2. Here we compare the computational complexity of (3.9), (3.10) and Algorithm 4.1 in implementing the first order SAV-DG scheme (3.4). We use P^1 polynomials with time step $\Delta t = 10^{-2}$ and meshes $N \times N$. The total CPU time and the orders of the CPU time relative to the number of unknowns are presented in Table 4.

Let $\mathcal{N} = 6N^2 + 1$ be the total number of unknowns. The results tell us that the computational complexity of (3.9) is $O(\mathcal{N}^2)$, but only $O(\mathcal{N})$ for (3.10) and Algorithm 4.1. The key for the $O(\mathcal{N})$ complexity lies in the sparsity of the coefficient matrix, however, (3.10) solves a larger system, and Algorithm 4.1 involves a pre-evaluation procedure. Still Algorithm 4.1 appears best among all three methods.

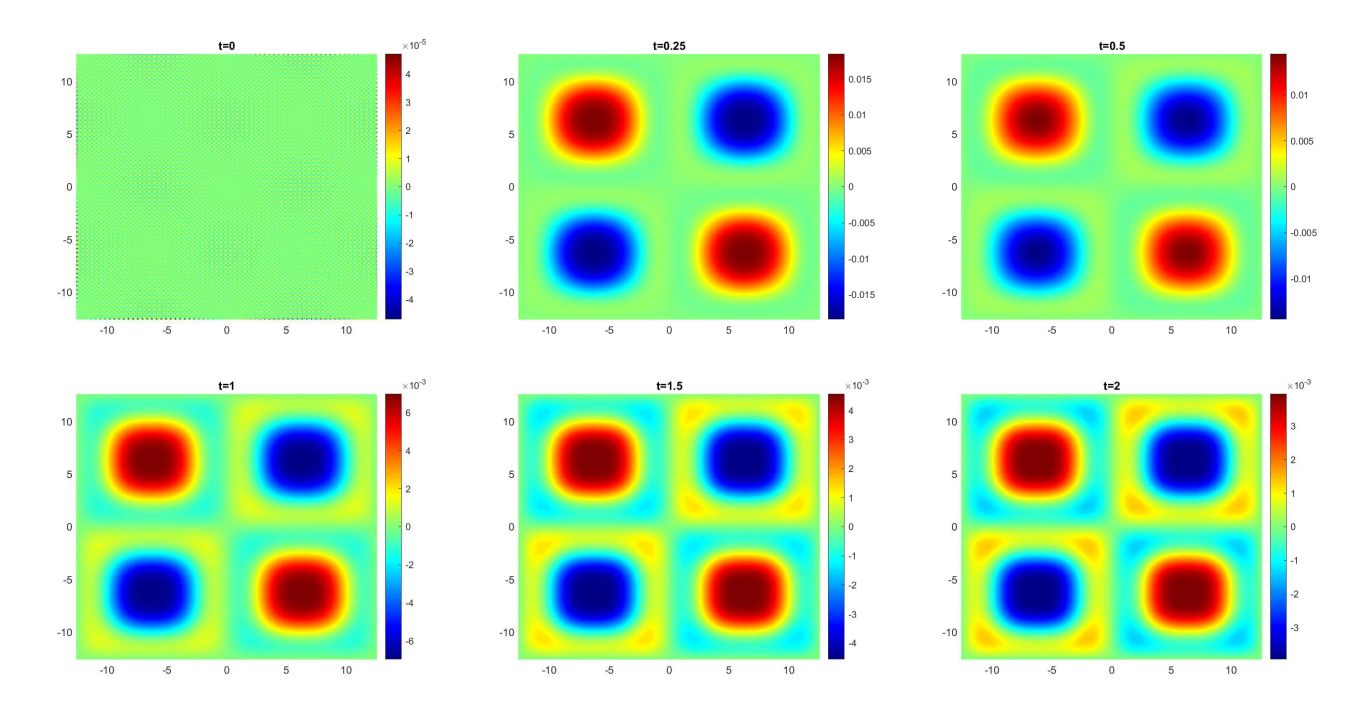


Figure 2. Evolution of the difference $u_h^n(x,y) - u(t^n,x,y)$ with $\Delta t = 2^{-2}$ and N = 64.

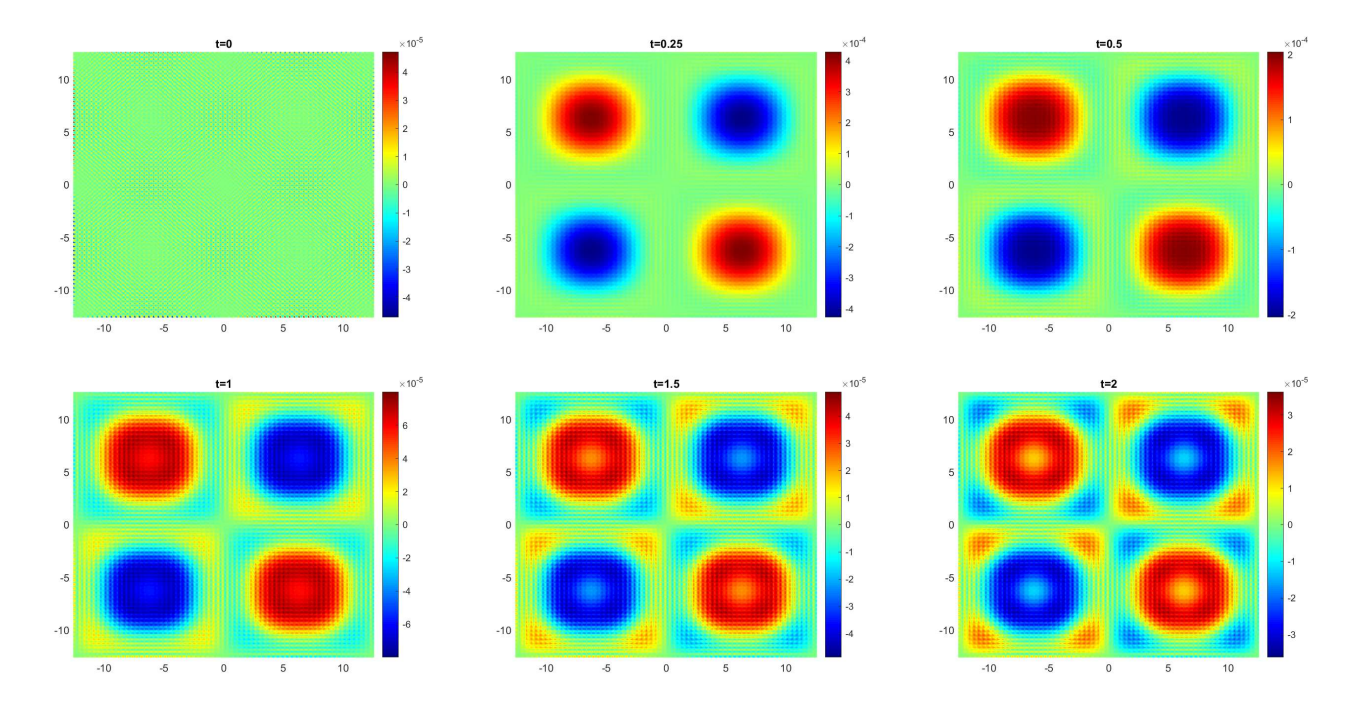


FIGURE 3. Evolution of the difference $u_h^n(x,y) - u(t^n,x,y)$ with $\Delta t = 2^{-5}$ and N = 64.

6. Concluding remarks

For a class of fourth order gradient flows, integration of the spatial discretization based on the penalty-free DG method introduced in [12] with the temporal discretization based on the SAV approach introduced in [21] to handle nonlinear terms led us to SAV-DG schemes. Such

method	N=8	N=16		N=32	2	N=64		
method	CPU time	CPU time	order	CPU time	order	CPU time	order	
(3.9)	3.46	16.58	1.13	157.58	1.63	2687.80	2.05	
(3.10)	2.70	9.79	0.93	38.10	0.98	155.07	1.01	
Algorithm 4.1	2.10	7.39	0.91	28.49	0.97	116.00	1.01	

Table 4. The CPU time in seconds with respect to meshes $N \times N$ at T = 0.1.

schemes inherit the energy dissipation property of the continuous equation irrespectively of the mesh and time step sizes. However, the resulting linear system involving unknowns (u,q) only, where q is an approximation of $\mathcal{L}=-\left(\Delta+\frac{a}{2}\right)u$, is rather expensive to solve due to the dense coefficient matrix. In this paper, we have developed hybrid SAV-DG algorithms in two steps: we (i) provide a procedure to pre-evaluate the auxiliary variable r^{n+1} in the piecewise polynomial space, and (ii) solve the resulting linear system with the obtained r^{n+1} . This procedure reduced the computational complexity of the CG solver to $O(\mathcal{N})$ from $O(\mathcal{N}^2)$; here \mathcal{N} is the total number of unknowns. We also presented several numerical examples to assess the performance of the hybrid SAV-DG algorithms in terms of accuracy and energy stability. Also the cost of the hybrid SAV-DG performing better as evidenced by our numerical results.

ACKNOWLEDGMENTS

This research was supported by the National Science Foundation under Grant DMS1812666.

APPENDIX A. PROOFS OF ENERGY DISSIPATION LAWS

Proof. (i) We first prove (3.7). From (3.4b), it follows

$$(D_t q_h^n, \psi) = A(D_t u_h^n, \psi). \tag{A.1}$$

Taking $\psi = q_h^{n+1}$ and $\phi = D_t u_h^n$ in (3.4a), when combined with (3.4c) we have

$$-\|D_{t}u_{h}^{n}\|^{2} = (D_{t}q_{h}^{n}, q_{h}^{n+1}) + (b(u_{h}^{n}), D_{t}u_{h}^{n})r^{n+1}$$

$$= \frac{1}{2}D_{t}\|q_{h}^{n}\|^{2} + \frac{\Delta t}{2}\|D_{t}q_{h}^{n}\|^{2} + 2r^{n+1}D_{t}r^{n}$$

$$= \frac{1}{2}D_{t}\|q_{h}^{n}\|^{2} + \frac{\Delta t}{2}\|D_{t}q_{h}^{n}\|^{2} + D_{t}|r^{n}|^{2} + \Delta t|D_{t}r^{n}|^{2},$$
(A.2)

which leads to the desired equality (3.7).

Next we show the uniqueness of the SAV-DG scheme (3.4). Let $(\tilde{u}, \tilde{q}, \tilde{r})$ be the difference of two possible solutions at $t = t_{n+1}$, then (A.2) is equivalent to

$$\frac{1}{\Delta t} \|\tilde{u}\|^2 + \|\tilde{q}\|^2 + 2|\tilde{r}|^2 = 0,$$

hence we must have $(\tilde{u}, \tilde{q}, \tilde{r}) = (0, 0, 0)$, leading to the uniqueness of the linear system (3.4), hence its existence since for a linear system in finite dimensional space, existence is equivalent to its uniqueness.

(ii) We first prove (3.8). From (3.5b), it follows

$$(D_t q_h^n, \psi) = A(D_t u_h^n, \psi). \tag{A.3}$$

Taking $\psi = q_h^{n+1/2}$ and $\phi = D_t u_h^n$ in (3.5a), when combined with (3.5c) we have

$$-\|D_t u_h^n\|^2 = (D_t q_h^n, q_h^{n+1/2}) + (b(u_h^{n,*})r^{n+1/2}, D_t u_h^n) = \frac{1}{2} D_t \|q_h^n\|^2 + D_t |r^n|^2.$$

Multiplying by Δt on both sides of this equality leads to (3.8).

Similar to (i), the existence of the SAV-DG scheme (3.5) is equivalent to its uniqueness, we let $(\tilde{u}, \tilde{q}, \tilde{r})$ be the difference of two possible solutions at $t = t_{n+1}$ again, then a similar analysis yields

$$\frac{1}{\Delta t} \|\tilde{u}\|^2 + \frac{1}{2} \|\tilde{q}\|^2 + |\tilde{r}|^2 = 0,$$

hence we must also have $(\tilde{u}, \tilde{q}, \tilde{r}) = (0, 0, 0)$, leading to the uniqueness of the scheme (3.5).

REFERENCES

- [1] G. Akrivis, B. Li, D. Li. Energy-decaying extrapolated RK–SAV methods for the Allen–Cahn and Cahn–Hilliard equations. SIAM Journal on Scientific Computing, 41(6):A3703–A3727, 2019.
- [2] G. J. B. van den Berg, L. A. Peletier and W. C. Troy. Global branches of multi-bump periodic solutions of the Swift-Hohenberg equation. *Arch. Rational Mech. Anal.*, 158:91–153, 2001.
- [3] G. Dee and W. Saarloos. Bistable systems with propagating fronts leading to pattern formation. *Phys. Rev. Lett.*, 60:2641–2644, 1988.
- [4] M. Dehghan and M. Abbaszadeh. The meshless local collocation method for solving multi-dimensional Cahn-Hilliard, Swift-Hohenberg and phase field crystal equations. *Eng. Anal. Bound. Elem.*, 78:49–64, 2017.
- [5] P. C. Fife and M. Kowalczyk. A class of pattern-forming models. J. Nonlinear Sci., 9:641–669, 1999.
- [6] H. Gomez and X. Nogueira. A new space-time discretization for the Swift–Hohenberg equation that strictly respects the Lyapunov functional. *Commun. Nonlinear Sci. Numer. Simulat.*, 17(12):4930–4946, 2012.
- [7] Y. Gong, J. Zhao and Q. Wang. Arbitrarily high-order linear energy stable schemes for gradient flow models. J. Comput. Phys., 419:109610, 2020.
- [8] Y. Gong, J. Zhao and Q. Wang. Arbitrarily high-order unconditionally energy stable SAV schemes for gradient flow models. *Computer Physics Communications*, 249:107033, 2020.
- [9] Y. Gong, J. Zhao and Q. Wang. Arbitrarily high-order unconditionally energy stable schemes for thermodynamically consistent gradient flow models. SIAM Journal on Scientific Computing, 42(1):B135–B156, 2020.
- [10] Jan S. Hesthaven and Tim Warburton. *Nodal Discontinuous Galerkin Methods: Algorithms, Analysis, and Applications*. Springer Publishing Company, Incorporated, 1st edition, 2007.
- [11] H. G. Lee. A semi-analytical Fourier spectral method for the Swift-Hohenberg equation. Computers & Mathematics with Applications, 74:1885–1896, 2017.
- [12] H. Liu and P. Yin. A mixed discontinuous Galerkin method without interior penalty for time-dependent fourth order problems. J. Sci. Comput., 77:467–501, 2018.
- [13] H. Liu and P. Yin. Unconditionally energy stable DG schemes for the Swift-Hohenberg equation. J. Sci. Comput., 81:789–819, 2019.
- [14] H. Liu and P. Yin. Unconditionally energy stable DG schemes for the Cahn-Hilliard equation. *Journal of Computational and Applied Mathematics*, 390:113375, 2021.
- [15] H. Liu and P. Yin. High order unconditionally energy stable RKDG schemes for the Swift-Hohenberg equation. Journal of Computational and Applied Mathematics, 407:114015, 2022.
- [16] D. Morgan, J. H. P. Dawes. The Swift-Hohenberg equation with a nonlocal nonlinearity. Physica D: Nonlinear Phenomena, 270(1):60–80, 2014.

- [17] L. A. Peletier and V. Rottschäfer. Pattern selection of solutions of the Swift-Hohenberg equation. *Physica D: Nonlinear Phenomena*, 194(1):95–126, 2004.
- [18] L. A. Peletier and W. C. Troy. Spatial patterns described by the extended Fisher-Kolmogorov (EFK) equation: kinks. Differ. Integral Equ., 8:1279–1304, 1995.
- [19] Bèatrice Riviére. Discontinuous Galerkin Methods for Solving Elliptic and Parabolic Equations. Society for Industrial and Applied Mathematics, 2008.
- [20] Chi-Wang Shu. Discontinuous Galerkin methods: General approach and stability. Numerical Solutions of Partial Differential Equations, S. Bertoluzza, S. Falletta, G. Russo and C.-W. Shu, Advanced Courses in Mathematics CRM Barcelona, pages 149–201, 2009. Birkhauser, Basel.
- [21] J. Shen, J. Xu and X. Yang. The scalar auxiliary variable (SAV) approach for gradient flows. *J. Comput. Phys.*, 353:407–416, 2018.
- [22] J. R. Shewchuk. An introduction to the conjugate gradient method without the agonizing pain. 1994.
- [23] J. Swift and P. C. Hohenberg. Hydrodynamic fluctuations at the convective instability. *Physical Review A*, 15:319–328, 1977.
- [24] X. Yang. Linear, first and second order and unconditionally energy stable numerical schemes for the phase field model of homopolymer blends. *J. Comput. Phys.*, 302:509–523, 2016.
- [25] X. Yang, J. Zhao and Q. Wang. Numerical approximations for the molecular beam epitaxial growth model based on the invariant energy quadratization method. J. Comput. Phys., 333:104–127, 2017.
- [26] X. Yang, J. Zhao, Q. Wang and J. Shen. Numerical approximations for a three components Cahn-Hilliard phase-field model based on the invariant energy quadratization method. *Math. Models Methods Appl. Sci.*, 27:1993–2030, 2017.
- [27] J. Zhao, Q. Wang and X. Yang. Numerical approximations for a phase field dendritic crystal growth model based on the invariant energy quadratization approach. *Int. J. Numer. Methods Eng.*, 110(3):279–300, 2017.
- [28] J. Zhou and X. Dai. An energy-stable pseudospectral scheme for Swift-Hohenberg equation with its Lyapunov functional. *Thermal Science*, 23:975–982, 2019.
 - † Iowa State University, Department of Mathematics, Ames, IA 50011 $Email\ address$: hliu@iastate.edu
- [‡] Multiscale Methods and Dynamics Group, Computer Science and Mathematics Division, Oak Ridge National Laboratory, Oak Ridge, Tennessee 37831, USA.

Email address: yinp@ornl.gov